Int J Earth Sci (Geol Rundsch) (2012) 101:221–238
DOI 10.1007/s00531-011-0672-0

ORIGINAL PAPER

Amphibole-derived evidence of medium *P/T* metamorphic ratio in Alpujárride and Federico "H*P*" units (Western Betic-Northern Rif, Spain and Morocco): possible interpretations

M. D. Ruiz Cruz · C. Sanz de Galdeano

Received: 13 August 2010 / Accepted: 6 May 2011 / Published online: 20 May 2011

Abstract The significance of zoned Ca-amphibole found in metapelites, quartzites, and synfolial veins of the Internal Zone of the Betic-Rif range (Federico units from Northern Rif and Alpujárride units from Western Betic) in the Alpine tectono-metamorphic evolution of these units is discussed for first time. Typical Al-rich metapelites from both areas show assemblages consisting of white mica and chlorite, with sporadic kyanite and chloritoid. Nevertheless, in the Rif zone, phyllites and synfolial veins of Permo-Triassic units show the assemblage pumpellyite + epidote + actinolite. In the Jubrique area (Betic zone), Ca-rich phyllites, fine-grained quartzites, and quartz veins show assemblages consisting of Ca-amphibole, plagioclase, epidote, titanite, chlorite, and quartz. The Al-in-amphibole thermobarometer defines clockwise pressure–temperature paths with a range of prograde temperatures and pressures between 272°C-1.2 kbar and 484°C-3.2 kbar for the Federico unit and between 274°C-1.1 kbar and 620°C-6.1 kbar in the Jubrique unit. Amphiboles from both areas define prograde pressure–temperature paths typical of Barrovian-type metamorphism. This finding contrasts with previous estimates, which deduced high-pressure conditions in both areas. The described amphiboles indicate metamorphic conditions similar to those found in the tectonically deepest complex (Veleta complex) of the Betic Internal Zone and suggest formation during a medium *P/T* Alpine event, which has not been previously identified in the Alpujárride complex.

Keywords Amphibole · Betic cordillera · Internal zone · Metamorphism · Thermobarometry

M. D. Ruiz Cruz (✉)
Departamento de Química Inorgánica, Cristalografía y Mineralogía. Facultad de Ciencias, Universidad de Málaga, 29071 Málaga, Spain
e-mail: mdruiz@uma.es

C. Sanz de Galdeano
Instituto Andaluz de Ciencias de la Tierra. Facultad de Ciencias, CSIC-Universidad de Granada, 18071 Granada, Spain

Introduction

Pressure–temperature (*P–T*) conditions of metamorphism are more easily determined for the metamorphic peak and the retrograde path. In contrast, the prograde evolution is generally poorly constrained. This is also the case for the metamorphic formations of the Internal Zone of the Betic-Rif range, in which indicators of the early compressional events have been largely destroyed during the late decompressional tectonic development related to exhumation.

For medium-grade metamorphic conditions, the *P–T* prograde paths can be accurately estimated using chemical data derived from two main mineral groups: garnets and amphiboles. Garnet is common in medium-grade metapelites but, unfortunately, it is absent in the younger metapelitic units (phyllites) of the Alpujárride complex and in the intermediate units between the Maláguide (Ghomaride, in Morocco) and the Alpujárride (Sebtide, in Morocco) complexes treated here. In contrast, amphibole, although in very low amounts, is widespread in both areas and can be used for geothermobarometry.

Amphibole is a monitor of polyphase metamorphic evolution due to its compositional sensitivity to changing *P* and *T*. Numerous studies have shown that increasing metamorphic grade in Ca-amphiboles causes an increase in Ti, Al, Na, and K and a parallel decrease in Si (e.g., Raase 1974; Brown 1977; Spear 1980; Robinson et al. 1982; Holland and Blundy 1994; Bellot et al. 2003). The Na and

Al content in amphibole increases as a function of both *P* and *T*. ^{IV}Al and Na in *M*(4) are a measure of *P* of metamorphism, while increasing (Na + K) at the *A*-site, and ^{VI}Al is considered to reflect *T* of metamorphism (Laird and Albee 1981; Ernst and Liu 1998; Zenk and Schulz 2004). This chemical control, associated with the instability of plagioclase, leads to the formation of Na amphibole (glaucophane) in high-*P* terrains (blueschists). In addition, zoned amphiboles generally preserve several stages (prograde and/or retrograde) of their *P–T* history, due to incomplete reequilibration (e.g., Bachman and Dungan 2002; Schulz et al. 2001; Vogl 2003). For this reason, several thermometers and barometers have been calibrated during the last decades with the aim of using the amphibole composition in reconstructions of the *P–T* paths (e.g., Raase 1974; Graham and Powell 1984; Blundy and Holland 1990; Mäder and Berman 1992; Anderson and Smith 1995).

In previous papers, we have described in detail the mineral assemblages in amphibole-bearing rocks from the intermediate units of the Rif (Ruiz Cruz et al. 2010) and from the Alpujárride complex (Ruiz Cruz 2010), but we have not discussed their possible significance. In this work, we compare the *P–T* paths deduced from zoned amphiboles in units intermediate between the Ghomaride and Sebtide complexes (Federico units, Northern Rif) and of typical Alpujárride units (Jubrique unit, Western Betics) with (1) the *P–T* paths (that were mainly based on Al-rich assemblages) previously proposed for the Alpine metamorphic evolution in these same areas, (2) in other areas of the Betic-Rif range, and (3) the Veleta and Mulhacén complexes (based on data from metapelites and metabasites), which outcrop in the central and eastern part of the Betic cordillera. The results strongly contrast with those from previous data.

Most amphibole data from both areas are published, but a summary of data is included here, since amphiboles from both formations have not been previously compared.

Geological setting review

The Betic-Rif cordillera (SE Spain and N Morocco) makes up part of the peri-Mediterranean Alpine orogenic system (Fig. 1a). This cordillera has traditionally been divided (Fallot 1948) into an external domain, consisting of Triassic to Middle Miocene sedimentary rocks, and an internal domain, composed mainly of Palaeozoic to Tertiary metamorphic rocks. Successive reviews of the geology of these cordilleras (e.g., Egeler and Simon 1969; Kampschuur and Rondel 1975; Fontboté and Vera 1983; Sanz de Galdeano 1990) follow these subdivision criteria.

The Betic-Rif Internal domain has been generally subdivided into three nappe complexes named, from top to bottom: the Maláguide (Betic)-Ghomaride (Rif) (Durand-Delga 1968), the Alpujárride (Betic)-Sebtide (Rif) (Van Bemmelen 1927), and the Nevado-Filábride (Egeler 1963), which is only present in the Betic area (Fig. 1b). In addition, intermediate units between the Maláguide-Ghomaride and the Alpujárride-Sebtide complexes have been described along the cordillera (Sanz de Galdeano et al. 2001). These are especially well represented in the Rif (Federico units) and also in the westernmost part of the Betic cordillera.

The original position of the Betic-Rif Internal Zone has been a matter of discussion. We support the idea that it was situated in an eastern position within the Western Mediterranean, as has been indicated by many authors (Andrieux et al. 1971; Wildi 1983; Boillot et al. 1984; Sanz de Galdeano 1990, among others), situated in an intermediate position between the African and the European plates and formed the AlKaPeCa domain (Bouillin et al. 1986). This name is the acronym of Alboran, Kabylia, Peloritani Mountains, and Calabria in allusion to the present places where the original domain crops out.

After extensional stages along the Triassic and the Cretaceous, from Late Cretaceous, and particularly during the Paleogene, the AlKaPeCa domain was subjected to compression. Probably, the first stage of deformation corresponded to subduction, when parts of the Mesozoic oceanic basins were destroyed. Subduction continued in a complex process of collision, perhaps alternating with periods of extension and uplifts, as suggested by the relative positioning of the units. This process continued approximately to the end of the Oligocene, when the opening of the Argelo-Provençal basin in the western Mediterranean commenced. The opening of this basin was related to a new phase of subduction occurring in the NW part of the African Plate (the present arc existing between Sicily and the South of the Italian Peninsula is a rest of this subduction). With the opening of the Argelo-Provençal basin, the AlKaPeCa domain was destroyed and their remnants moved in different directions. The Betic-Rif Internal Zone was pushed toward the West, to its present position, while at the same time its eastern part suffered the extension that created the Alboran Sea, as the Western end of the Argelo-Provençal basin.

Interpretation of the processes involved in the exhumation has been the source of controversy. There is no general agreement about the tectonic regime and the timing of exhumation, and very different tectonic and geodynamic models have been proposed. These include contractional (e.g., Tubía et al. 1992; Simancas and Campos 1993), extensional (e.g., Platt and Vissers 1989; García-Dueñas et al. 1992; Vissers et al. 1995; Platt et al. 1996), or alternation of both regimes (e.g., Bakker et al. 1989; Azañón et al. 1997; Balanyá et al. 1997).

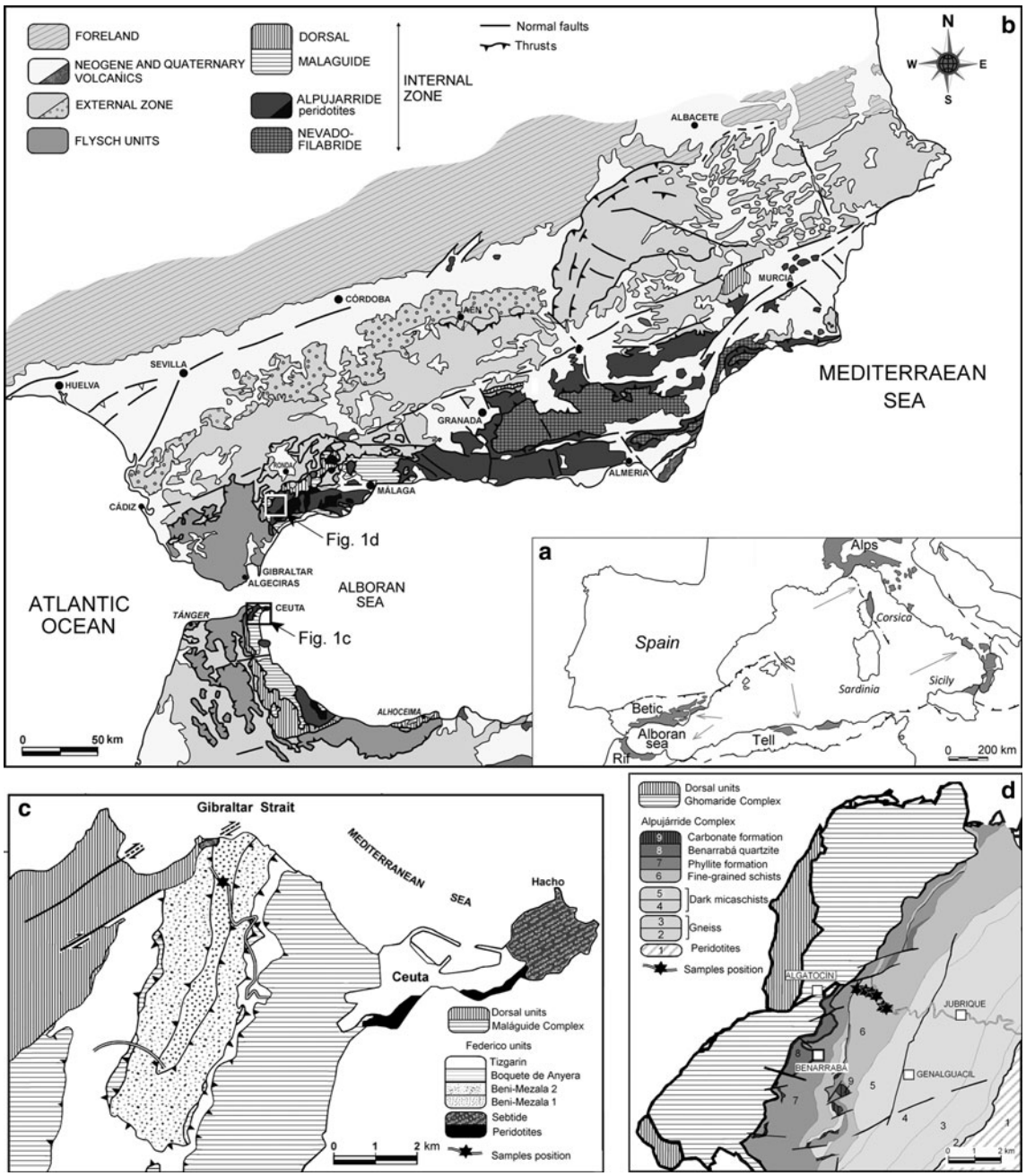

Fig. 1 **a** Simplified tectonic map of the Mediterranean region showing the distribution of the Internal Zone core complexes. **b** Tectonic map of the Betic-Rif-Alborán orogenic system in the western Mediterranean and location of the study areas. **c** Tectonic map of the northern area of the Rif, modified from Kornprobst and Durand-Delga (1985), and location of the samples used in this work (*star*). **d** Simplified geological map of the Jubrique area, modified from Olmo Sanz del et al. (1987), and location of the samples used in this work (*stars*)

Summary of lithology and metamorphic patterns of the internal zone complexes

The lowest metamorphic complexes of the Betic cordillera (the Nevado-Filábride complex in Fig. 1b) are at present called the Veleta and Mulhacén complexes (Puga et al. 2002a, b). These complexes are made up of a stack of metamorphic thrust nappes that crop out in the central and eastern part of the Betic cordillera. Both complexes include a pre-Permo-Triassic basement mainly formed by graphite-rich schists and minor marbles and subvolcanic lenses, and a Permo-Triassic, Triassic and younger cover, consisting of quartzites, marbles, schists, and orthogneisses. The Mulhacén sequence includes, in addition, an ophiolitic unit

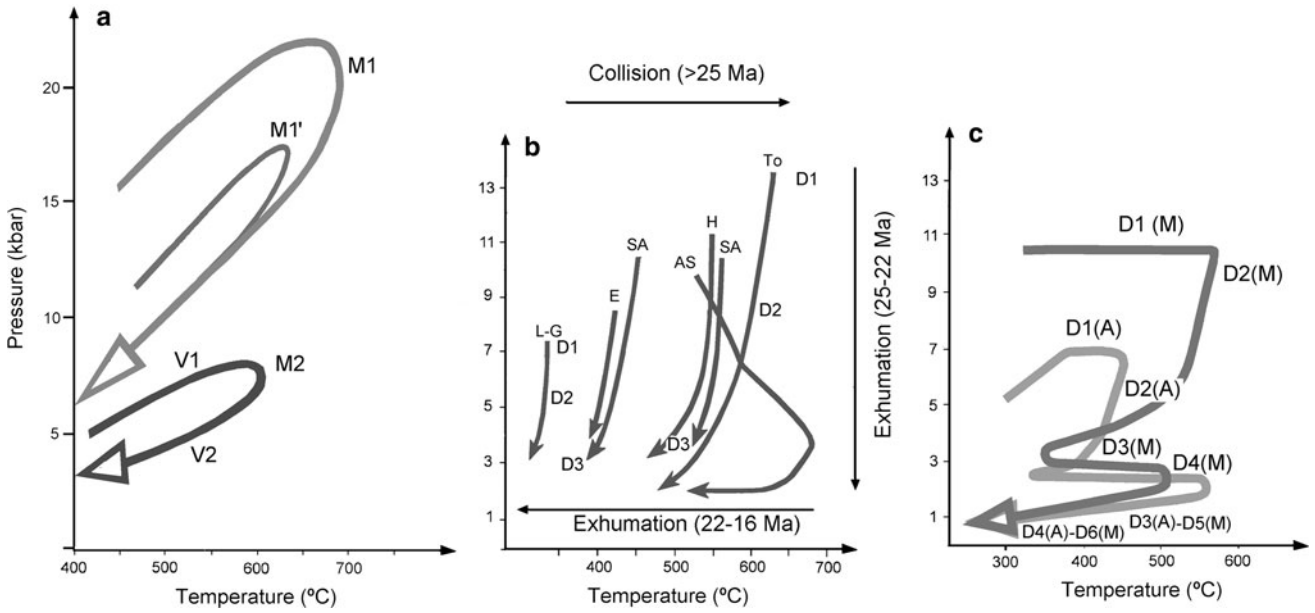

Fig. 2 *P–T* paths previously proposed for the Veleta (*V*) and Mulhacén (*M1*, *M1′* and *M2*) complexes (**a**), Alpujárride units (**b**), and Alpujárride (*A*) and Mulhacén (*M*) complexes (**c**). **a** Simplified from Puga et al. (2002a). *M1* Mulhacén complex from the central Betics (Sierra Nevada). *M1′* Mulhacén complex from the eastern-central part of the Betics (Sierra de los Filabres). **b** Simplified from Soto and Platt (1999). *L-G* Lújar-Gádor units and *E* Escalate units (*lower* Alpujárride units), *SA* Salobreña units and *H* Herradura units (*Intermediate* Alpujárride units), *To* Torrox units (*upper* Alpujárride units). **c** Simplified from De Jong (1991) for the eastern zone of the cordillera (Sierra de los Filabres, Sierra Alhamilla and Sierra de las Estancias). In **b** and **c**, *D* Main deformation stages

made up of gabbro- and basalt-derived eclogites and amphibolites as well as a sedimentary sequence consisting mainly of calc-schists and marbles. The Alpine metamorphism in these complexes has been subdivided into two main events: a Late Cretaceous–Paleocene (91–52 Ma) eo-Alpine event and a Late Eocene–Oligocene (48–25 Ma) meso-Alpine event (see Puga et al. 2002a, b and references therein). Nevertheless, the two complexes display contrasting metamorphic patterns. In the Veleta complex both the eo-Alpine and the meso-Alpine events developed under intermediate *P* conditions originating at their climax albite-epidote-amphibolite facies (Fig. 2a). In the Mulhacén complex, the eo-Alpine event developed under eclogite facies conditions, which varied between 15 and 17 kbar and ~600°C and 21–22 kbar and 650–700°C in several areas of the complex. This event was followed by a retrogression stage, leading to glaucophane-schist facies assemblages. The meso-Alpine event was characterized by albite-epidote-amphibolite facies conditions (Fig. 2a).

Rocks belonging to the Alpujárride-Sebtide complex are exposed along more than 400 km from the western part of the Málaga province to the Cartagena region (in the SE of Spain) and in the Northern part of the Rif (Fig. 1b). This complex includes several superimposed tectono-metamorphic units (Almagro-Carrascoy, Lújar-Gádor, Blanca-Almijara, and Güájares). Metamorphic grade increases from the bottom to the top of the pile. The lithostratigraphic sequence within each unit comprises the following formations, from bottom to top: (a) a micaschist formation, which locally includes gneisses and migmatites at its base with an assumed pre-Permian age; (b) a gray to bluish-gray fine-grained schist or phyllite formation thought to be Permo-Triassic; (c) a carbonate formation, dated as Middle to Late Triassic; (d) some units may contain younger formations of uncertain significance.

The Alpujárride complex shows plurifacial Alpine metamorphism. The deduced *P–T* paths in different units from this complex document a two-stage metamorphic evolution. Relicts of eclogitic assemblages in metabasites from the Blanca unit (Tubía and Gil Ibarguchi 1991) and carpholite-bearing assemblages in metapelites from the Güajares unit (Goffé et al. 1989; Azañón and Goffé 1997) indicate that high-pressure–low-temperature (H*P*-L*T*) metamorphic conditions characterized the initial phase of Alpine metamorphism. During the second stage, low-pressure–high-temperature (L*P*-H*T*) assemblages overprinted the earlier assemblages. An increase in temperature during the last stages of the exhumation of these rock types, indicating heating during decompression, has been described in rocks from the Alboran Sea (Platt et al. 1998). The first H*P*/L*T* event is usually associated with the early crustal-thickening stage (Goffé et al. 1989; Tubía and Gil Ibarguchi 1991) and the L*P*-H*T* event as characterizing the isothermal decompression (Goffé et al. 1989; Tubía et al. 1992; García-Casco and Torres-Roldán 1996; Azañón et al. 1997; Balanyá et al. 1997). The decompression segment of

the *P–T* paths bears a direct relation, according to some authors (García-Casco and Torres-Roldán 1996; Orozco et al. 1998), to the development of the S_2 (Sp) schistosity. Some *P–T* paths for different Alpujárride units are shown in Fig. 2b. Despite the polyphased metamorphic history of the Alpujárride complex, closure ages cluster in a narrow range between 23.4 and 15.5 Ma, most of them in the 19–20 Ma age range, only reflecting the exhumation stage.

According to Bakker et al. (1989), De Jong (1991, 1993), and others, the relation of mineral growth with respect to deformation phases showed that the tectono-metamorphic evolution of the Alpujárride and Mulhacén complexes was rather similar in the eastern zone of the cordillera. Both nappe complexes experienced H*P* conditions during early Alpine tectonics, when deformation structures with similar kinematic significance were formed. H*P* metamorphism gives way to L*P* conditions concomitant with cooling and was followed by reheating during younger Alpine movements (Fig. 2c).

The Maláguide-Ghomaride complex is comprised of: (a) phyllites and graywackes with minor limestone and metaconglomerate, with an Ordovician–Silurian (or older) age; (b) limestones, chert, and radiolarite rocks, dated as Devonian-Early Carboniferous; (c) Permo-Triassic red beds formation with conglomerates, sandstones, and lutites; and (d) a carbonate sequence with members from Triassic to Eocene age. The Maláguide-Ghomaride rocks have undergone Alpine metamorphism ranging from the diagenesis to the deepest anchizone (Ruiz Cruz and Rodríguez Jiménez 2002) in the Permo-Triassic red beds. The Paleozoic series preserve clear Variscan orogenic features showing greenschists-facies metamorphism (e.g., Chalouan and Michard 1990; Ruiz Cruz and Sanz de Galdeano 2010). The exposures of this complex are largely limited to the western Betics (North and East of Málaga) and to the northern Rif (Fig. 1b). Intermediate units between the Maláguide-Ghomaride and the Alpujárride-Sebtide complexes consist of a series of thinned tectonic slices including a Paleozoic basement with uniform characteristics throughout the tectonic pile and a Permo-Triassic to Triassic cover. Increasing metamorphic conditions characterize the passage from the upper Maláguide-like slices to the lower Alpujárride-like slices (Ruiz Cruz et al. 2005, 2006).

Study areas

The intermediate units from the Rif (Federico units) have been considered as upper Sebtide units (Bouybaouène 1993; Kornprobst 1974) or as units intermediate between the Ghomaride and the Sebtide complexes (Didon et al. 1973; Sanz de Galdeano et al. 2001). The Federico units are well exposed near Ceuta (Fig. 1c), where they are tectonically overlain by the Ghomaride units. Four tectonic units have been differentiated in this area, which are, from top to bottom: Tizgarín, Boquete de Anyera, Beni Mezala 2, and Beni Mezala 1 (Durand-Delga and Kornprobst 1963). All these units show similar normal stratigraphic sequences: Carboniferous metagraywackes at the bottom, Permo-Triassic metapelites, and Triassic quartzites, and carbonates at the top. The transition from the upper unit (Tizgarín) to the lower units is marked by a change in color from red to blue in the metapelites and an increase in metamorphic grade.

The Federico units were sampled along two traverses through the entire Beni Mezala antiform. The location of the sampling itineraries and of the samples used for this work is shown in Fig. 1c. Although sampling was carried out through the entire antiform, only phyllites and the enclosed veins found in the Beni Mezala sequence at the northern part of the outcrop (between N35°54′36.4″–W05°22′29.1″ and N35°54′28.4″–W05°22′26.6″) are used here. The samples are considered to correspond to the Beni Mezala 1 unit, but field criteria did not allow the unambiguous distinction of the Beni Mezala 1 and Beni Mezala 2 units in the Ceuta area.

The Jubrique unit (which can be considered as equivalent to the Güajares unit) was sampled following the itinerary shown in Fig. 1d. Sampling was carried out through the entire Jubrique unit, but only samples from zone 6 (between N36°34′07.4″–W5°14′38.8″ and N36°34′27″–W5°15′9″), representative from the several amphibole-bearing lithotypes, are used for this work. In contrast to the previous descriptions, which define the samples from this unit as biotite-bearing schists, we found that the rocks have a dominant phyllitic (and minor quartzite) composition, which varies in color from deep blue in the upper parts to dark gray in the lower ones. Minor amounts of biotite have been identified only in one sample.

Summary of the petrography of the amphibole-bearing and related rocks

Federico units

In the tectonically lower Federico Unit (Beni Mezala 1), amphiboles appear in synfolial quartz-rich veins strongly deformed by the main schistosity (Fig. 3a). Veins are enclosed in Permo-Triassic blue phyllites and quartzites. Quartz veins contain irregular and variably sized aggregates of fine-grained green minerals, generally distinguishable at the field scale. The mineral assemblage includes, in addition to quartz and minor plagioclase, epidote, amphibole, pumpellyite, muscovite, vermiculite,

titanite, and magnetite. Amphibole is dominant in some veins, whereas epidote dominates in others. Pumpellyite is always a minor constituent. Amphibole generally appears to be concentrated in the vein areas between quartz and epidote as thin needles, commonly associated with pumpellyite (Fig. 4a). Zonation in amphibole was not observed at the scale of the petrographic microscope and the back-scattered images (Fig. 5a). Nevertheless, chemical zoning was evident in some grains, as shown below.

Other veins from this area consist of quartz, with large kyanite crystals filling millimeter-sized veinlets oblique to the vein boundaries. Kyanite occurs as strongly deformed prismatic grains and as smaller unoriented grains around the prisms. White micas occur in several textural settings with kyanite. In some areas, white mica appears to have grown in equilibrium with kyanite, showing straight boundaries between the two phases and a lack of reaction signals. Nevertheless, most white mica pervasively replacing kyanite is fine-grained and intergrown with chlorite, at the kyanite-quartz boundaries. Chloritoid is scarce and appears as small prisms, in apparent equilibrium with kyanite and the first-generation white mica (Ruiz Cruz et al. 2010).

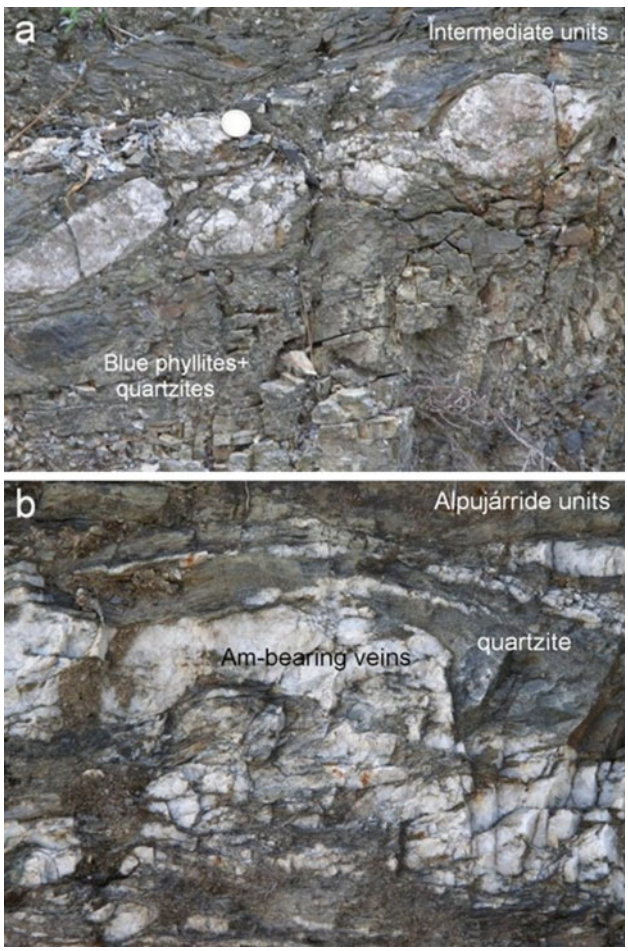

Fig. 3 Amphibole-bearing quartz veins from the Beni Mezala 1 unit (Northern Rif) (**a**) and from the Jubrique unit (Western Betic) (**b**)

Alpujárride unit

The rocks studied are blue-to-dark gray phyllites and quartzites that contain numerous quartz- and minor plagioclase-rich lens-shaped veins of variable size, from a few centimeters to several decimeters wide, parallel to and deformed by the event that formed main schistosity, similar to those found in the Federico units (Fig. 3b).

Amphibole-bearing assemblages are widespread in this unit (Ruiz Cruz 2010), although amphibole appears in minor amounts. It is common in quartz-rich synfolial veins, indistinguishable, at the field scale, from those containing kyanite. In veins, amphibole is concentrated in irregular domains, where small, unoriented radial grains predominate. Colorless amphibole is the most abundant in veins, although rims are present in some grains (Fig. 4b). In the back-scattered images, colorless amphibole shows a darker contrast than the green amphibole rims (Fig. 5b). Locally, Ca-rich phyllites consist of quartz + plagioclase + K-feldspar + muscovite + amphibole + epidote + titanite + magnetite + ilmenite + chlorite. Ca-bearing silicates and chlorite are concentrated in millimeter-sized pre-Sp domains (Figs. 4c and 5c). In quartzites, amphibole forms lens-shaped aggregates, with elongation parallel to the main schistosity, scattered through the sample (Fig. 4d). Progressive zonation from colorless to blue-to-green is commonly observed. In addition, a reverse zonation is observed in some grains, where darker cores are rimmed by lighter rims.

Typical Al-rich phyllites contain, in contrast, synfolial quartz-rich veins with kyanite and rare chloritoid, similar to those found in the Federico units. Kyanite and chloritoid are also common in phyllites. Chloritoid appears as very small prisms pre-, syn-, and post-Sp.

Summary of amphibole and associate minerals chemistry

Although numerous analyses of amphibole and associated phases have been previously published (Ruiz Cruz 2010; Ruiz Cruz et al. 2010), we will summarize here the main results.

Amphibole

Amphibole analyzed in the Federico and Alpujárride units is Ca-amphibole according to the IMA nomenclature (Leake et al. 1997). Formulae were calculated from the electron microprobe (EMP) data, following Schumacher

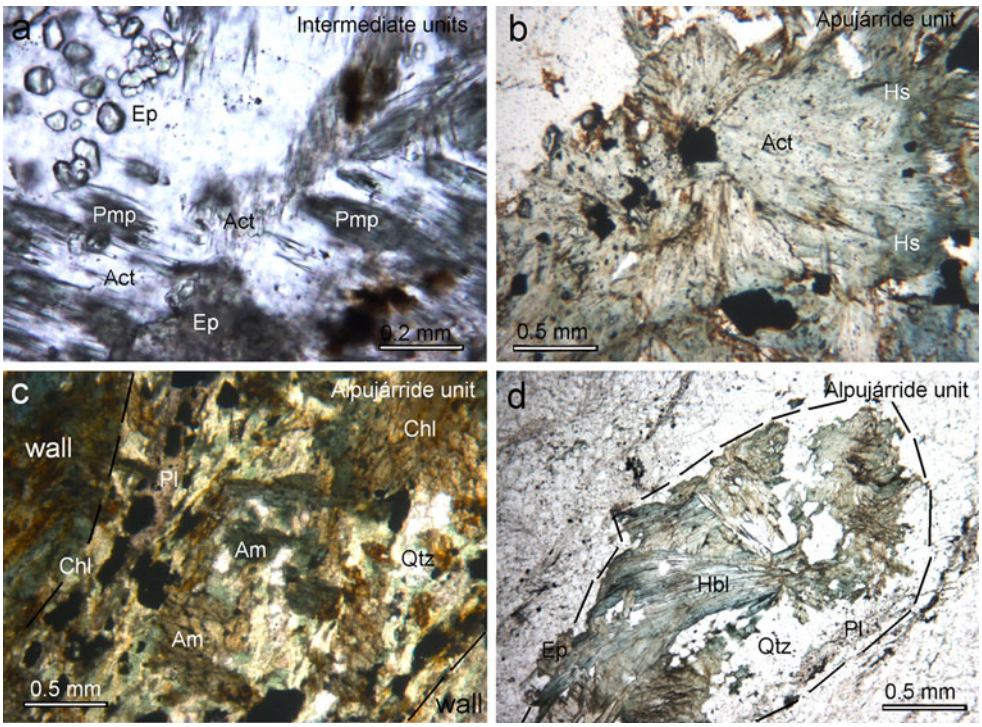

Fig. 4 Photomicrographs of amphibole-bearing samples. **a** Actinolite (*Act*) + pumpellyite (*Pmp*) + epidote (*Ep*) assemblage from quartz-rich vein of the Beni Mezala 1 unit (plane-polarized light). **b** Radial amphibole with a well-developed actinolite (*Act*) core and a green–blue rim of hastingsite (*Hs*), from quartz-vein of the Jubrique unit (plane-polarized light). **c** Syn-Sp segregation filled by quartz (*Qtz*), plagioclase (*Pl*), K-feldspar, amphibole (*Am*), ilmenite and chlorite (*Chl*) in phyllite from the Jubrique unit (plane-polarized light). **e** *Lens-shaped* domain of amphibole + plagioclase (*Pl*) + epidote (*Ep*) parallel to Sp in quartzite from the Jubrique unit (plane-polarized light). Mineral symbols according to Kretz (1983)

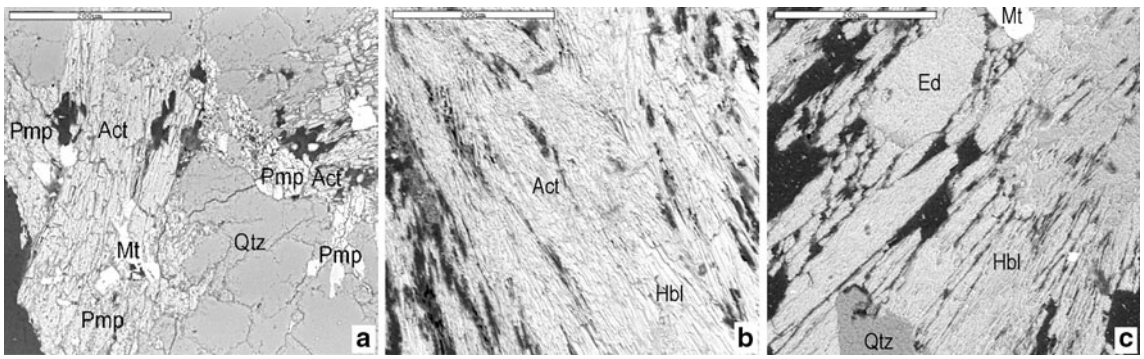

Fig. 5 *Back-scattered images* showing: **a** the textural relations in veins from the Federico unit; **b** zoning in radial amphibole from veins of the Jubrique unit; and **c** intergrowths of Hbl and Ed in phyllite from the Jubrique unit

(1997, 2007); Holland and Blundy (1994) and by normalization to 13 cations (13eCNK). Formulae normalized to 13 cations have been used in the representations and in Table 1. In the Federico unit, most amphibole is tremolite and actinolite, with minor magnesiohornblende in some rims (Fig. 6; Table 1, analyses 1 and 2). In some rarer grains, the outermost rim is also actinolite. In the Alpujárride unit, chemical data show that zonation is characterized by a decrease in the Si content toward the rim of the grains followed, in some grains, by a new increase in Si (Table 1, analyses 3–4, 4–7, and 8–10). As shown in Fig. 6, amphibole composition includes the complete magnesioactinolite and magnesiohornblende fields, reaching the tschermakite field, and the Fe-richer terms. A second population, represented by rarer analyses, shows higher ^{A}(Na + K) contents and plots on the edenite, pargasite, and ferrohastingsite fields. The number of edenite and pargasite analyses increases considerably, where the formulae are calculated using the methods of Schumacher (1997, 2007) or Holland and Blundy (1994).

Amphibole shows significant chemical correlations, some of which are shown in Fig. 7. In amphiboles from both areas, Si and Al show a strong negative correlation (Fig. 7a), indicating that zonation is marked by the increase in Al, parallel to the decrease in Si. Si shows a positive correlation with Mg and a negative correlation with total Fe, indicating a Fe-enrichment in the overgrowths. A positive correlation is shown by Al and K (Fig. 7b), with two different trends, marked by pargasite and hastingsite. A positive correlation is also observed between Al and Na, although edenite deviates from the general trend (Fig. 7c). A negative correlation is shown by Si and Ti, and a positive correlation between K and Cl, with Cl content (>4% in some cases) increasing considerably in some hastingsite

Table 1 Selected EMP analyses of amphibole normalized to 13 cations (13eCNK) and calculated *P–T* values

	Federico unit				Alpujárride unit					
	Vein		Vein		Phyllite			Quartzite		
	Core	Rim	Core	Rim	Core		Rim	Core		Rim
	1	2	3	4	5	6	7	8	9	10
SiO_2	53.77	52.62	54.34	38.24	47.05	41.61	46.96	49.94	44.22	50.55
TiO_2	0.10	0.15	0.04	0.44	0.33	0.53	0.25	0.24	0.54	0.24
Al_2O_3	2.74	4.51	1.72	11.81	7.89	11.26	11.94	5.99	10.44	5.12
Cr_2O_3	0.00	0.05	0.02	0.02	0.00	0.02	0.03	0.00	0.01	0.02
FeO	8.86	9.79	8.96	24.64	14.91	17.81	16.44	12.44	17.07	12.67
MnO	1.20	1.01	0.38	0.66	0.53	0.54	0.50	0.55	0.55	0.53
MgO	17.25	16.57	17.81	4.49	11.59	8.36	8.43	14.77	10.72	15.13
CaO	12.34	12.21	12.25	11.55	11.72	11.98	10.99	12.35	12.05	12.68
Na_2O	0.25	0.34	0.21	1.03	1.33	1.95	0.99	0.54	0.93	0.46
K_2O	0.08	0.14	0.16	1.99	0.41	0.95	0.43	0.16	0.37	0.16
Cl	n.d.	n.d.	0.05	4.13	0.28	0.23	0.31	0.22	0.38	0.14
F	n.d.	n.d.	0.24	0.31	0.95	1.76	0.49	0.18	0.20	0.22
Total	96.61	97.43	96.19	99.37	97.00	96.99	97.78	97.42	97.59	97.92
Si	7.66	7.45	7.78	6.19	7.05	6.51	6.94	7.21	6.56	7.27
^{IV}Al	0.34	0.55	0.22	1.81	0.95	1.49	1.06	0.79	1.44	0.73
ΣT	8.00	8.00	8.00	8.00	8.00	8.00	8.00	8.00	8.00	8.00
^{VI}Al	0.12	0.20	0.07	0.44	0.44	0.59	1.02	0.23	0.39	0.14
Ti	0.01	0.02	0.00	0.05	0.04	0.06	0.03	0.03	0.06	0.03
Fe^{3+}	0.34	0.20	0.28	0.52	0.21	0.00	0.13	0.51	0.77	0.46
Fe^{2+}	0.72	0.69	0.79	2.81	1.65	2.33	1.91	0.99	1.35	1.06
Mn	0.14	0.12	0.05	0.09	0.07	0.07	0.06	0.07	0.07	0.07
Mg	3.66	3.50	3.80	1.08	2.59	1.95	1.86	3.18	2.37	3.24
ΣC	5.00	5.00	5.00	5.00	5.00	5.00	5.00	5.00	5.00	5.00
Ca	1.88	1.85	1.88	2.00	1.88	2.00	1.74	1.91	1.92	1.95
Na	0.12	0.15	0.12	0.00	0.12	0.00	0.26	0.09	0.09	0.05
ΣB	2.00	2.00	2.00	2.00	2.00	2.00	2.00	2.00	2.00	2.00
Na	0.00	0.00	0.00	0.32	0.27	0.59	0.02	0.06	0.18	0.08
K	0.01	0.03	0.03	0.41	0.08	0.19	0.08	0.03	0.07	0.03
ΣA	0.01	0.03	0.03	0.73	0.34	0.78	0.10	0.09	0.25	0.11
F	n.d.	n.d.	0.07	0.16	0.13	0.11	0.15	0.08	0.10	0.10
Cl	n.d.	n.d.	0.01	1.14	0.24	0.47	0.12	0.05	0.10	0.03
X_{Mg}	0.84	0.84	0.83	0.28	0.61	0.46	0.49	0.76	0.64	0.75
Classification	Act	Mg-Hbl	Act	Cl-Hast	Mg-Hbl	Fe-Ed	Fe-Hbl	Mg-Hbl	Mg-Hbl	Mg-Hbl
T	406	447	392	659	371	446	601	492	590	484
P	1.8	2.8	1.5	6.3	3.1	3.6	5.4	3.4	5.4	3.0

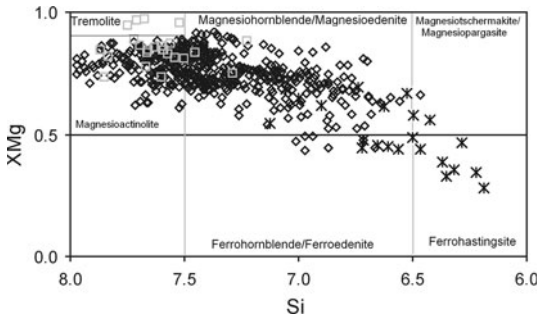

Fig. 6 Compositional fields and classification of the Ca-amphiboles in the $Mg/(Mg + Fe^{2+})$ versus Si diagram. *Squares* Tremolite, actinolite, and hornblende from the Beni Mezala 1 unit. *Diamonds* Actinolite-tschermakite series from the Jubrique unit. *Crosses* Edenite, pargasite, and hastingsite from the Jubrique unit

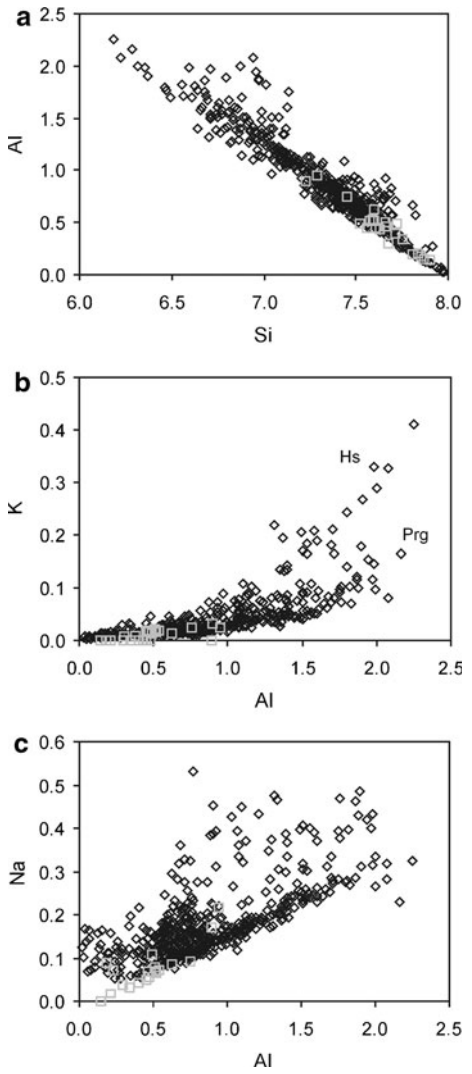

Fig. 7 Chemical plots showing the most significant correlations in the studied amphiboles. *Squares* Tremolite, actinolite, and hornblende from the Beni Mezala 1 unit. *Diamonds* Actinolite-tschermakite series from the Jubrique unit

analyses. As a whole, all these trends indicate that zoned Ca-amphiboles grew at increasing *P* and *T*.

Plagioclase

In the Federico unit, plagioclase analyses correspond to Na-rich terms ($\sim An_{11}$) in phyllites and to slightly Ca-richer terms ($\sim An_{18}$) in veins (Table 2, analyses 1 and 2). In the Alpujárride rocks, plagioclase is scarce in quartz-rich veins, more abundant in quartzites, and highly abundant in phyllites. In veins, plagioclase shows predominant composition of An_{50} (Table 2, analysis 3) and minor grains with composition of An_{73}. In quartzites, the composition of plagioclase is more homogeneous, with a mean composition of An_{58} (Table 2, analysis 4). In amphibole-bearing phyllites, feldspars (plagioclase and K-feldspar) appear as lens-shaped aggregates, almost completely replaced by white mica and filling the segregations. In most cases, fine intergrowths of plagioclase and K-feldspar are present. In the segregation walls, plagioclase shows mean compositions of An_{38} and An_{62}. Important zonation is observed in segregation-filling plagioclase, where depletion in Ca is evident at the boundaries with Ca–Al silicates (amphibole and epidote) (Table 2, analysis 5).

Epidote

Epidote is more abundant in the Federico unit. Although all analyses correspond to Fe-rich terms, Fe increases toward the crystal rim (Table 2, analyses 6 and 7). In the Alpujárride unit, Fe-rich (and in some cases REE-rich) cores in zoned epidote grains from amphibole-bearing domains are rimmed by zoisite-enriched areas (Table 2, analyses 8 and 9). This type of zonation (increase in the Al content) is generally attributed to increasing *T* (Beiersdorfer and Day 1995; Bird et al. 1988). Maximum Al content is present in fine fibers of epidote found in the innermost part of the segregations.

Pumpellyite

Pumpellyite is present only in the Federico unit. The quality of the analyses is difficult to ascertain because of the size of the pumpellyite grains and the possible variations in the number of hydroxyls and trivalent ions. Although analyses clearly contaminated by adjacent quartz or phyllosilicates have been excluded, a slight Si excess or a slight Ca deficiency is observed when the formulae are calculated on the basis of 16 cations and 24.5 oxygens. Nevertheless, the analyses are within the range $93.8 \pm 2.0\%$, considered acceptable by Schiffmann and Day (1999). Two pumpellyite populations have been identified. Pumpellyite from actinolite-bearing samples is Fe-rich,

Table 2 Selected EMP analyses of plagioclase, epidote, and pumpellyite

	Plagioclase						Epidote					Pumpellyite	
	Federico unit		Alpujárride unit				Federico unit		Alpujárride unit			Federico unit	
	Phyllite 1	Vein 2	Vein 3	Quartz. 4	Phyllite 5		Core 6	Rim 7	Core 8	Rim 9		10	11
SiO_2	63.91	60.34	56.49	55.09	69.26	SiO_2	37.87	37.41	34.67	38.9	SiO_2	37.92	38.30
TiO_2	0.02	0.02	0.10	0.00	0.09	TiO_2	0.04	0.04	0.21	0.15	TiO_2	0.12	0.29
Al_2O_3	22.68	23.70	27.34	27.66	18.87	Al_2O_3	25.78	22.26	19.32	25.21	Al_2O_3	21.33	23.70
FeO	0.33	0.33	0.24	0.18	0.45	Fe_2O_3	10.46	14.95	13.24	10.12	Cr_2O_3	0.05	0.02
MnO	0.00	0.00	0.01	0.00	0.05	Mn_2O_3	0.41	0.44	0.11	0.12	Fe_2O_3	9.04	5.48
MgO	0.02	0.02	0.00	0.49	0.00	MgO	0.04	0.01	0.29	0.07	Mn_2O_3	0.27	0.27
CaO	2.14	3.23	10.41	11.60	0.36	CaO	23.31	22.95	12.94	24.26	MgO	3.28	3.29
Na_2O	8.50	7.37	5.22	4.69	11.04	La_2O_3			5.24		CaO	22.27	22.38
K_2O	1.48	1.48	0.12	0.39	0.26	Ce_2O_3			9.43		Na_2O	0.07	0.12
Total	99.21	99.58	99.64	100.12	100.38	Nd_2O_3			3.03		K_2O	0.02	0.13
						Na_2O	0.02	0.02	0.39	0.04	Total	94.31	94.00
						K_2O	0.03	0.00	0.11	0.10			
						Total	98.05	97.99	98.98	98.98			
Atomic proportions for O = 8						*Atomic proportions for O = 12.5*					*Atomic proportions for O = 24.5*		
Si	2.86	2.78	2.55	2.49	3.01	Si	2.99	3.00	3.11	3.01	Si	6.07	6.14
Al	1.20	1.29	1.46	1.47	0.99	Al	2.39	2.11	2.04	2.30	Al	4.02	4.47
Fe	0.01	0.01	0.01	0.01	0.02	Fe^{3+}	0.59	0.87	0.99	0.65	Ti	0.01	0.04
Mg	0.00	0.00	0.00	0.03	0.00	ΣY	2.99	2.98	3.03	2.95	Fe^{3+}	0.86	0.01
Ca	0.10	0.16	0.50	0.56	0.02	Fe^{2+}	0.03	0.03	0.00	0.00	Fe^{2+}	0.35	0.72
Na	0.74	0.66	0.48	0.41	0.95	Mn	0.02	0.03	0.01	0.01	Mn	0.03	0.03
K	0.08	0.09	0.01	0.02	0.01	Mg	0.00	0.00	0.04	0.01	Mg	0.79	0.79
						Ca	1.97	1.97	1.24	2.01	Ca	3.82	3.83
An	11.10	17.62	51.00	57.00	2.00	La	n.d.	n.d.	0.17	n.d.	Na	0.02	0.00
Ab	79.76	72.76	48.00	41.00	97.00	Ce	n.d.	n.d.	0.31	n.d.	K	0.00	0.02
Or	9.14	9.61	1.00	2.00	1.00	Nd	n.d.	n.d.	0.10	n.d.			
						Na	0.00	0.00	0.07	0.01			
						K	0.00	0.00	0.01	0.01			
						ΣW	2.03	2.03	1.90	2.03			
						XAl	80.00	71.00	0.67	0.78			

whereas pumpellyite from actinolite-free veins and from phyllites shows higher Al contents (Table 2, analysis 11 and 12).

Phyllosilicates

In the Federico unit, fine-grained pale-green chlorite is abundant in pumpellyite-free phyllites. Analyses show variations in composition, mainly affecting the Si contents (2.64–2.77 apfu), which suggest that chlorite growth occurred at variable *T*. Nevertheless, chlorite shows rather homogeneous Mg/(Fe + Mg) ratios (0.70–0.77), characteristic of clinochlore (Table 3, analysis 1). Chlorite is very rare in veins, which contain instead vermiculite (Table 3, analysis 2).

In the Alpujárride unit, several texturally different types of chlorite have been identified in amphibole-bearing rocks, which show some variations in chemical composition. In contrast, chlorite from Al-rich phyllites shows homogeneous compositions. As a whole, chlorite from amphibole-bearing rocks shows notably lower X_{Mg} (0.46–0.58) than does chlorite from Al-rich phyllites ($\sim$0.70) (Table 3, analyses 3 and 4).

Muscovite from phyllites of the Federico and Alpujárride units shows limited substitution toward celadonite (Table 3, analyses 5 and 8). In contrast, white micas from kyanite-bearing veins include Ms with variable Si content according to the textural position (up to 3.16 apfu, Table 3, analysis 6, 7, and 9) and margarite pervasively replacing kyanite (Table 3, analysis 10).

Table 3 Selected EMP analyses of phyllosilicates and chloritoid

	Trioctahedral phyllosilicates				White micas						Chloritoid		
	Federico unit		Alpujárride unit		Federico unit			Alpujárride unit			Federico unit	Alpujárride unit	
	Chl Phyllite 1	Vrm Vein 2	Chl Phyllite 3	Chl Phyllite 4	Ms Phyllite 5	Ms Vein 6	Ms Vein 7	Ms Phyllite 8	Ms Vein 9	Mrg Vein 10	Vein 11	Phyllite 12	Phyllite 13
SiO_2	28.54	43.56	25.99	26.98	46.63	48.16	46.70	46.11	47.29	29.81	24.07	22.88	23.28
TiO_2	0.00	0.12	0.20	0.00	0.30	0.19	0.31	0.40	0.00	0.04	41.09	0.00	0.12
Al_2O_3	24.58	17.04	18.87	23.83	35.49	34.23	34.39	35.83	34.70	45.43	0.07	37.17	38.20
FeO	12.22	11.13	28.15	15.80	2.88	2.82	3.31	2.64	2.90	0.48	19.55	29.01	27.68
MnO	0.25	0.38	14.91	0.42	0.00	0.00	0.00	0.00	0.12	0.00	1.08	1.74	1.90
MgO	24.08	16.85	0.34	21.87	0.74	0.88	0.77	0.34	0.80	0.09	4.09	0.49	0.50
CaO	0.00	2.03	0.08	0.13	0.00	0.69	0.24	0.34	0.11	10.39	0.49	0.20	0.02
Na_2O	0.25	0.47	0.34	0.02	1.51	0.75	1.38	0.86	0.73	1.43	0.23	0.02	0.00
K_2O	0.00	0.25	0.01	0.00	9.24	8.57	8.56	10.04	10.67	0.54	0.59	0.07	0.20
Total	89.92	91.86	88.89	89.06	96.80	96.29	95.66	96.56	97.31	88.21	91.45	91.58	91.91
Atomic proportions for O = 11					*Atomic proportions for O = 11*						*Atomic proportions for 8 cations*		
Si	2.72	3.09	2.76	2.66	3.07	3.16	3.07	3.05	3.13	2.14	Si 1.97	1.94	1.96
^{IV}Al	1.28	0.91	1.24	1.34	0.93	0.84	0.93	0.95	0.87	1.86	Al 3.96	3.78	3.83
^{VI}Al	1.47	0.51	1.11	1.43	1.81	1.81	1.74	1.85	1.83	1.99	Ti 0.00	0.00	0.01
Ti	0.00	0.01	0.02	0.00	0.02	0.01	0.02	0.02	0.00	0.00	Fe^{3+} 0.05	0.34	0.24
Fe^{2+}	0.97	0.66	2.50	1.30	0.16	0.15	0.18	0.15	0.16	0.03	Fe^{2+} 1.29	1.71	1.70
Mn	0.02	0.02	0.03	0.04	0.00	0.00	0.00	0.00	0.01	0.00	Mn 0.07	0.04	0.04
Mg	3.42	1.79	2.36	3.22	0.07	0.09	0.07	0.03	0.08	0.01	Mg 0.49	0.22	0.24
Σoct.	5.88	2.99	6.02	5.99	2.06	2.05	2.02	2.05	2.07	2.03	Ca 0.04	0.02	0.00
Ca	0.00	0.16	0.01	0.01	0.00	0.05	0.02	0.03	0.01	0.80	Na 0.04	0.00	0.00
Na	0.05	0.06	0.07	0.00	0.19	0.10	0.18	0.11	0.09	0.20	K 0.06	0.01	0.02
K	0.00	0.02	0.00	0.00	0.77	0.72	0.72	0.85	0.90	0.05	X_{Mg} 0.26	0.11	0.12
Σint.	0.05	0.24	0.08	0.02	0.97	0.86	0.91	0.99	1.00	1.05			
X_{Mg}	0.78	0.73	0.49	0.71	0.30	0.38	0.28	0.17	0.32	0.25			

The formulae of chloritoid from kyanite-bearing veins of the Federico unit, calculated on the basis of 8 cations and with ferric iron estimated as 4-(Al + Ti), reveal a maximum Mg/(Fe + Mg) ratio of 0.26 (Table 3, analyses 11). Chloritoid from amphibole-bearing rocks of the Alpujárride unit shows more homogeneous Mg/(Fe + Mg) values on the order of 0.11 (Table 3, analyses 12–13).

Summary of thermobarometric estimations

In previous papers, we compared the *P–T* estimates deduced from amphibole- and pumpellyite-bearing rocks with those deduced from associated Al-rich phyllites and Ky-bearing veins. In Al-rich phyllites from both areas, the mineral assemblage consists of quartz, sodic plagioclase, muscovite, chlorite, rare paragonite, and either pyrophyllite (in the Federico unit) or kyanite (in the Alpujárride unit). This is a very common assemblage in Al-rich pelitic rocks, but well-calibrated thermobarometers do not exist. Estimates of *P* and *T*, realized using the crystal-chemical properties of chlorite and muscovite from the Federico unit (Ruiz Cruz et al. 2010), indicated a *T* range of 280 to 350–400°C for $P < 3$ kbar. In the Alpujárride unit, presence of minor chloritoid permitted the use of the chlorite-chloritoid thermometer of Vidal et al. (1999), which provided *T* of ~500°C (Ruiz Cruz 2010).

In kyanite-bearing veins, there are few phases in equilibrium for unambiguously estimating the *P–T* conditions with THERMOCALC, and the estimates of Ruiz Cruz et al. (2010) ($T = 386 \pm 20$°C and $P = 4.3$–5.1 kbar) for the Federico unit must be considered as an approximation. As a consequence, our estimations were mainly based on the changes in amphibole composition in zoned grains.

The use of Ca-rich silicates (amphibole, pyroxenes, pumpellyite, epidote, etc.) in *P–T* determinations has been

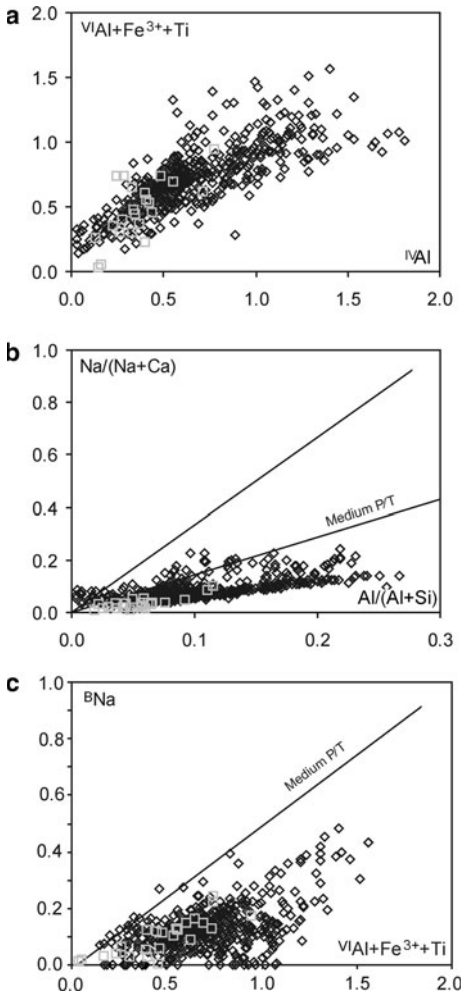

Fig. 8 Plot of the analyzed amphiboles on the Laird and Albee (1981) diagrams $^{VI}Al + Fe^{3+}+Ti$ versus ^{IV}Al (**a**), Na/(Na + Ca) versus Al/(Al + Si) (**b**), and on the Laird et al. (1984) diagram ^{B}Na versus $^{VI}Al + Fe^{3+} + 2Ti$ (**c**). In **a** the actinolite-tschermakite series shows a trend similar to that shown by the Barrowian-type amphiboles. In **b** most analyses plot below the low *P/T* metamorphic gradient. In **c** most amphiboles plot below the barroisite line, in the fields of low and medium *P*. Points near or over this line correspond to Na–Ca-amphiboles, where the ^{B}Na content is probably enhanced due to the normalization method. *Squares* Tremolite, actinolite, and hornblende from the Beni Mezala 1 unit. *Diamonds* Actinolite-tschermakite series from the Jubrique unit

generally restricted to metabasites (Bucher and Frey 2002; Robinson and Bevins 1999), since these assemblages are rarely present in pelitic rocks. It has been demonstrated, however, that growth-zoned Ca-amphiboles have a high potential for *P–T* reconstructions (e.g., Bégin and Carmichel 1992; Triboulet 1992; Schulz et al. 1995).

In amphibole-bearing rocks from the Federico units, chemical characteristics of amphibole points to increasing but low *T* and *P* of formation. In contrast, in the Jubrique units, chemical zonation points to important increase in *T* and *P* during amphibole growth. Some classical diagrams (Laird and Albee 1981; Laird et al. 1984) have been successively used to distinguish between pressure facies series of metabasites. Where represented in the ($^{VI}Al + Fe^{3+}+Ti$) versus ^{IV}Al diagram (Fig. 8a), the whole of our amphibole analyses shows a trend similar to that shown by the Barrovian-type amphiboles (Laird and Albee 1981; Zenk and Schulz 2004), with amphibole from the Federico unit showing a more restricted field. The Na/(Na + Ca) versus Al/(Al + Si) plot (Fig. 8b) of amphibole compositions shows a linear trend, mainly below the line defining the low *P*-metamorphism. Again amphibole from intermediate units occupies a narrower field. Similarly, in the ^{B}Na versus ($^{VI}Al + Fe^{3+} + 2Ti$) diagram, most amphiboles plot below the barroisite line, in the fields of the low- and medium-*P* amphiboles (Fig. 8c).

Although we previously used the Anderson and Smith (1995) barometer combined with the Holland and Blundy (1994) thermometer (Ruiz Cruz 2010), in this work, we will only use the results obtained with the thermobarometer of Gerya et al. (1997), modified by Zenk and Schulz (2004). As a whole, this thermobarometer yields a range of prograde *T* between 272 and 484°C, for a *P* range from 1.2 to 3.2 kbar for amphiboles from the Federico units. The range is between 274 and 620°C and between 1.1 and 6.1 kbar in the Jubrique unit. Na-rich amphiboles (edenite, pargasite and hastingsite) were excluded from the *P–T* determinations, since in most cases they provided unrealistic *T* and *P* values (Ruiz Cruz 2010).

Detailed *P–T* evolution deduced from a complete set of chemical profiles indicated that in quartz-rich veins from the Federico units, the *P–T* paths mainly reflect the prograde evolution, except in some scarce grains, where a retrograde path is also evident (e.g., Fig. 9a). Amphibole from the Jubrique unit shows well-defined retrogressive paths (e.g., Fig. 9b). The deduced general *P–T* paths suggest a first stage of amphibole (actinolite or tremolite) growth with dominant increase in *T* (up to ~400°C), followed by hornblende with high actinolite component (Federico units) and by hornblende, tschermakite, pargasite, and hastingsite growth (Jubrique unit), at increasing *P* and *T* (Fig. 9c). The retrogressive paths are generally parallel to the prograde ones.

Comparing the *P–T* conditions determined in Federico units from the Rif, with those determined in the Jubrique Alpujárride unit, it seems evident that the rocks from the Jubrique area underwent higher *P* and *T*. This is in accordance with the previous interpretations, since lower metamorphic conditions for the Rif (Federico units) formations related to the Jubrique area had also previously been deduced (Didon et al. 1973; Sanz de Galdeano et al. 2001), and the Rif units were considered by these authors as intermediate between the Maláguide and the Alpujárride complexes.

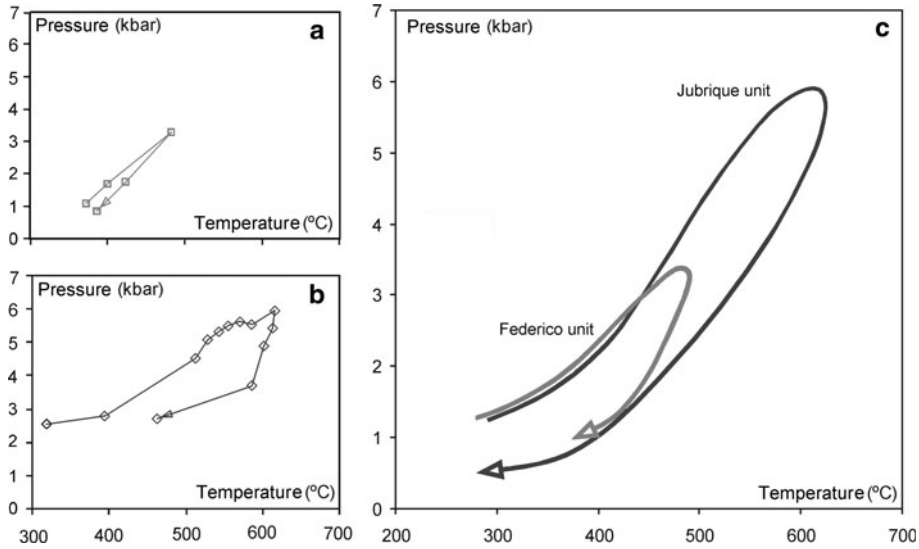

Fig. 9 *P–T* paths deduced from two zoned amphiboles of the Federico (**a**) and the Jubrique (**b**) units. **c** General *P–T* paths defined by the whole of the amphiboles from the Federico (*light gray line*) and from the Jubrique unit (*dark gray line*), estimated using the thermobarometer of Zenk and Schulz (2004) from more than 40 zoned grains

Discussion

An important point concerns to the time of formation of amphibole-bearing assemblages in veins and phyllites from the intermediate (Federico) and Alpujárride (Jubrique) units. Ages of metamorphic episodes in the Alpujárride complex have been extensively investigated by means of both high- (SHRIMP U/Pb dating on zircons) and low- ($^{40}Ar/^{39}Ar$ dating on white micas) *T* isotopic closure systems. Nevertheless, a large amount of radiometric data cluster at the Early Miocene times (19–23 Ma), which only record the latest metamorphic stage. Indeed, the extremely rapid rock uplift and concomitant cooling rates that characterize the extensional stage of Alpine orogeny produced telescoping of isotopic ages as most thermochronometric closure temperatures are within the 600 ± 100°C cooling range. This results in very precise ages for the rapid rock uplift/cooling but cloaks the earlier history of the rock complexes, as pointed out by Zeck and Whitehouse (1999). As a consequence, other (mainly textural) criteria have been used for determining the sequence of mineral growth.

Parageneses in synfolial veins from Alpujárride-Sebtide units of the Betic-Rif zone have been systematically considered as having formed during the crustal-thickening H*P*-L*T* event (Azañón and Goffé 1997; Bouybaouène et al. 1995; Michard et al. 1997). Deformation of amphibole-bearing veins (Fig. 3) and textural relations at the scale of the thin sections (Fig. 4) clearly indicate that amphibole grew before- and probably during the development of the main schistosity (Sp or S2). Sp has been previously used (Balanyá et al. 1993, 1997) as a time marker since, according to this author, it appears to be the unique deformation phase that developed between the H*P*-L*T* and the later L*P*-H*T* stages. Nevertheless, following this criterion, amphibole formation in intermediate and Alpujárride units described in this work must be related to the first compressional episode, responsible for the H*P* assemblages.

The pumpellyite- and amphibole-bearing assemblages appear restricted, in the units studied, to quartz-feldspathic veins and metapelites richer in Ca than the most common Al-rich phyllites. These compositional differences led to the formation of mineral assemblages considered as very rare in phyllites (Schumacher 2007). These rock types differ from typical Al-rich phyllites, where Al-rich phases (e.g., pyrophyllite, kyanite, chloritoid) dominate; they also differ from classical metabasic rocks, where amphiboles are abundant and from classical calc-schists. In calc-schists from the central Alps, clinozoisite-, scapolite- and pyroxene-bearing assemblages develop at higher metamorphic grades (e.g., Kuhn et al. 2005). As a consequence, although data about the significance of zoned amphiboles in metabasic rocks (mainly ophiolite complexes) of very different ages and geotectonic settings are abundant in the literature, data about pumpellyite- or amphibole-bearing phyllites are very rare (e.g., Zen 1974; Nishimura et al. 2000; Vogl 2003; Krenn et al. 2004; Daczko et al. 2009) and generally correspond to geologic formations very different from those treated here. Curiously, and although the two zones studied here have been previously investigated in detail, data about these rock types and their metamorphic assemblages have been not described.

Previous estimates in the study areas

An H*P*/L*T* metamorphic event affecting the Permo-Triassic formations of the Federico units was reported in the study by Bouybaouène (1993). The *P–T* conditions characterizing the climax of this metamorphic event evolved, according to Bouybaouène (1993); Bouybaouène et al.

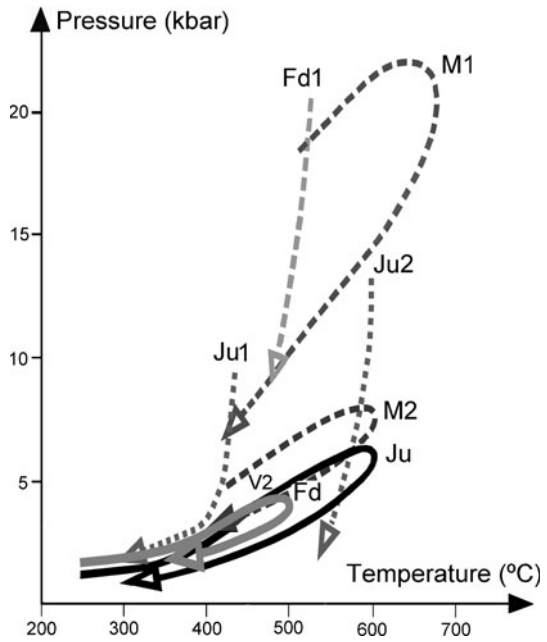

Fig. 10 Comparison of previous *P–T* paths deduced in the studied areas with our results. Fd1: *P–T* estimate for the lowermost Federico unit (Beni Mezala 1), from Bouybaouène (1993). Ju1 and Ju2: *P–T* estimates for phyllites and schists of the Jubrique area, from Azañón et al. (1995) and Balanyá et al. (1997). M1 and M2: *P–T* estimates for the Mulhacén complex; and V2: *P–T* estimates for the Veleta complex, from Puga et al. (2002a). Fd and Ju (*continuous lines*): *P–T* estimates for the lowermost Federico unit (Beni Mezala 1) and for the Jubrique unit, from this work

(1995) and Michard et al. (1997), from 300°C and 1–2 kbar in the uppermost Federico unit to the blueschist facies (430–450°C and 12–15 kbar) and to the eclogite facies (550°C and 20 kbar) in the deepest Beni Mezala 1 unit (Fd1 in Fig. 10). The *P–T* conditions of these units were deduced on the basis of the local presence of metamorphic assemblages containing sudoite, chloritoid, carpholite, and talc. X_{Mg} in chloritoid ranged between 0.30 and 0.50 according to these authors.

Ruiz Cruz et al. (2010) did not find carpholite in the area where amphibole-bearing parageneses appear (Beni Mezala 1 unit). In addition, chloritoid shows maximum of $X_{Mg} = 0.26$. These authors deduced maximum *T* of 386 ± 20°C and a poorly defined *P* interval going from 4.3 to 5.1 kbar for kyanite-bearing veins, where both kyanite and chloritoid probably formed from the breakdown of pyrophyllite and chlorite (Frey and Wieland 1975; Theye et al. 1992). Nevertheless, thermobarometric data based on amphibole composition indicate that maximum *T* reached 484°C, for *P* of 3.2 kbar, suggesting that pumpellyite persisted metastably at these physical conditions.

In the Jubrique unit, an Alpine H*P*/L*T* metamorphic event affecting the Permo-Triassic phyllite formation directly overlying, and in a part overlapping the samples used here (zone 7 in Fig. 1d) was reported in the studies by Azañón et al. (1995) and Balanyá et al. (1997). The metamorphic conditions of this formation are consistent with the *P–T* of collisional settings and were deduced again on the basis of the local presence of metamorphic assemblages containing pyrophyllite or kyanite, chloritoid, chlorite, and possible carpholite pseudomorphs. The estimated *P–T* conditions reached, according to these authors, *T* on the order of 400°C and $P > 8$ kbar (Ju1 in Fig. 10), notably lower than those estimated in the Rif. Chloritoid composition used in their determinations showed $X_{Mg} = 0.34$ and a $X_{Mg} = 0.75$ was assumed for carpholite, since fresh carpholite was not found. In schists underlying the phyllites studied here (top of zone 3 in Fig. 1d), the estimated metamorphic conditions were 600 ± 40°C and 11 ± 1 kbar (Balanyá et al. 1997) (Ju2 in Fig. 10), both formations suggesting a thermal gradient of ~18°C/km. Therefore, a H*P* metamorphic imprint in the rock unit studied here (zone 6 in Fig. 1d) was expected. However, no indications of carpholite were found despite careful inspection of many quartz veins. In addition, the several chloritoid generations showed uniform $X_{Mg} = 0.12$, notably lower than that used in previous estimations by Azañón et al. (1995). Textural evidence suggests that amphibole formed from chlorite, probably through the reaction chlorite + calcite + quartz = amphibole + anorthite + CO_2 + H_2O (Sharp and Buseck 1988).

Possible interpretations

At least three interpretations could explain the disagreement among previous determinations and the results presented here: (1) the bulk compositions of the amphibole-bearing rocks were such that H*P* assemblages did not develop; (2) the H*P* assemblages were completely overprinted by the M*P* assemblages; and (3) the units studied were not subjected to H*P* conditions. The first hypothesis is probably not correct, since Al-rich phyllites contain kyanite + chloritoid assemblages and bulk compositions appropriate for the formation of carpholite. Nevertheless, carpholite is lacking and chloritoid shows very low X_{Mg}. Moreover, the amphibole-bearing rocks contain Na-bearing amphiboles (edenite, pargasite, and hastingsite) suggesting that lack of glaucophane that would form at higher *P* conditions is not due to chemistry.

Amphiboles commonly preserve the successive stages of their *P–T* history, due to incomplete re-equilibration. Vogl (2003) described amphibole-bearing metapelites from northern Alaska, where preserved glaucophane relicts permitted the distinction between different metamorphic regimes. Given the relatively low *T* of the medium *P* event, we believe that the early H*P* stage, if it existed, would have been in evidence in at least some of the 700 amphiboles

analyzed. While the second hypothesis cannot be disproved, the available textural and chemical data suggest to us that the units studied never reached H*P* metamorphism conditions. Our results indicate that the main schistosity (S2 or Sp) formed after and probably during the M*P* event described here, and then, it cannot be used for unequivocally identifying the H*P* event, as previously suggested.

As shown in Fig. 10, the *P–T* paths determined from amphibole composition in the intermediate units of the Rif (Federico units) (Fd in Fig. 10) and in the Alpujárride units from the Western Betic (Ju in Fig. 10) strongly contrast with previous estimations for peak metamorphic conditions in these areas (Fd1 and Ju1 in Fig. 10). In contrast, the paths are very similar in shape and extent to those previously determined by Puga et al. (2002a, b) for the eo-Alpine event in the Veleta complex and for the meso-Alpine event in both the Veleta (V2 in Fig. 10) and the Mulhacén complexes (M2 in Fig. 10).

The eo-Alpine and meso-Alpine collisional events have been well characterized in the Nevado-Filabride complex as well as in other Alpine chains from metamorphic parageneses developed in basic rocks (e.g., Desmons 1989; Carrupt and Schlup 1998; Puga et al. 2002a). Moreover, this event has also been characterized in the Nevado-Filábride complex from chloritoid- and garnet-bearing parageneses in metapelitic rocks (Puga et al. 2002a, b). Differences in metamorphic conditions between the Veleta and the Mulhacén complexes were interpreted by Puga et al. (2002a) as evidence of different tectonic settings for these units throughout the pre-Alpine and eo-Alpine metamorphic events and that the Mulhacén complex overthrust the Veleta complex during the meso-Alpine event.

On the basis of these data, two very different processes could explain the metamorphic heterogeneities observed in the zones studied here, assuming that the thermobarometric estimations are correct: (1) a late-stage tectonic juxtaposition of rock units recording different *P*-peaks and (2) a second metamorphic episode (meso-Alpine), during which amphiboles grew, affected the studied units. Tectonic juxtaposition of rock units recording different *P*-peaks is common and has been invoked, for example, for explaining the discrepancies found in *P* conditions between eclogites and meta-sedimentary country rocks from the Western Alps (Bousquet 2008). Whereas this explanation is plausible for dismembered sequences of mafic rocks included in a metapelitic matrix, it seems difficult to reconcile pelitic sequences cropping out over larger areas (Fig. 1). The more plausible explanation is that amphiboles formed during a medium *P/T* Alpine event, which has not been previously identified in the Alpujárride complex. This would imply that exhumation, generally considered to be a continuous and nearly isothermal process, was interrupted by a new collisional event, as also observed in the Nevado-Filábride complex (Fig. 2c). Data presented here clearly indicate that the stages of deformation in the Alpujárride Complex and in the intermediate units with the Maláguide Complex are not totally defined till this moment and are probably more numerous and complex than assumed by many authors.

Conclusions

Previous estimates of the *P–T* conditions attained in Al-rich metapelites from the Federico units (Rif) and from the Jubrique units (Betics) were estimated from mineral assemblages typical of Al-rich metapelites (e.g., pyrophyllite, kyanite, chloritoid, and sporadic carpholite). These assemblages led to the identification of a H*P*-L*T* Alpine event, which has been assumed as the most important event characterizing the Alpujárride formations from the Betic-Rif range. Nevertheless, we have not found carpholite in the two "H*P*" areas studied, and *P–T* estimations based kyanite- and chloritoid-bearing paragenesis indicated maximum *T* of 400–500°C and *P* of 4–5 kbar.

Finding amphibole-bearing parageneses in formations from both areas permitted a more accurate determination of the physical conditions that characterize the Alpine collisional event. Our principal assumption is that successive stages of equilibrium with matrix assemblage were recorded in the zoned amphiboles. Zonation in amphibole suggests that the actinolite (and rarer tremolite) cores crystallized at relatively low *T* and *P* (from ~300°C and ~1 kbar) in both the intermediate units from the Rif and the Alpujárride units from the Western Betics. Amphibole followed a prograde metamorphic evolution up to a maximum of ~480 and ~3.2 kbar in the intermediate units and ~620°C and ~6.1 kbar in the Alpujárride units. Thus, the zoned amphiboles reflect a prograde evolution from L*P*-L*T* to M*P*-M*T*. The *P–T* paths derived here support those derived from Al-rich parageneses (Ruiz Cruz et al. 2010) as well as the transitional nature of the Federico units between the Ghomaride and the Sebtide complexes.

The physical conditions estimated for the main metamorphic episode in the rocks from this study are very different from those previously estimated in these areas. In contrast, the deduced *P–T* paths are similar to those characterizing the Veleta complex, suggesting that the assemblages described in this study formed during a second collisional event. These new data also suggest that the Alpujárride complex (as the Nevado-Filábride complex) consists of units that occupied very different tectonic settings during the Alpine phase of their tectono-metamorphic evolution.

Acknowledgments The authors are grateful to P. Horváth and to an unknown reviewer, whose comments, suggestions, and corrections have notably improved the manuscript. This study has received financial support from the Project CGL 2009-08186 (Ministerio de Ciencia e Innovación) and from the Research Group RNM-199 (Junta de Andalucía).

References

Anderson JL, Smith DR (1995) The effects of temperature and fO_2 on the Al-in-hornblende barometer. Am Miner 80:549–559

Andrieux J, Fontboté JM, Mattauer M (1971) Sur un modéle explicatif de l'Arc de Gibraltar. Earth Planet Sci Lett 12:191–198

Azañón JM, Goffé B (1997) Ferro- and magnesiocarpholite assemblages as record of high-P, low-T metamorphism in the central Alpujárrides, Betic Cordillera (SE Spain). Eur J Miner 9:1035–1051

Azañón JM, Balanyá JC, García-Dueñas V (1995) Registro metamórfico de alta presión-baja temperatura en la unidad de Jubrique e imbricaciones de Benarrabá (Cordillera Bético-Rifeña). Geogaceta 17:133–134

Azañón JM, Crespo-Blanc A, García-Dueñas V (1997) Continental collision, crustal thinning, and nappe forming during the pre-Miocene evolution of the Alpujarride Complex (Alboran Domain, Betics). J Struct Geol 19:1055–1071

Bachman O, Dungan MA (2002) Temperature-induced Al-zoning in hornblendes of the fish Canyon magma, Colorado. Am Miner 87:1062–1076

Bakker HE, Jong De, Helmers H, Biermann C (1989) The geodynamic evolution of the internal zone of the Betic Cordilleras (south-east Spain): a model based on structural analysis and geothermobarometry. J Metam Geol 7:359–381

Balanyá JC, Azañón JM, Sánchez-Gómez M, García-Dueñas V (1993) Pervasive ductile extension, isothermal decompression and thinning of the Jubrique unit in the Paleogene (Alpujarride Complex, western Betics, Spain). C R Acad Sci Paris 316:1595–1601

Balanyá JC, García-Dueñas V, Azañón JM (1997) Alternating contractional and extensional events in the Alpujarride nappes of the Alborán Domain (Betics, Gibraltar Arc). Tectonics 16:226–238

Bégin NJ, Carmichel DM (1992) Textural and compositional relationships of Ca-amphiboles in metabasites of the Cape Smith Belt, Northern Québec: implications for a miscibility gap at medium pressure. J Petrol 33:1317–1343

Beiersdorfer RE, Day HW (1995) Mineral parageneses of pumpellyite in low-grade mafic rocks. Geol Soc Am Spec Paper 296:5–27

Bellot JP, Triboulet C, Laverne C, Bronner G (2003) Evidence for two burial/exhumation stages during the evolution of the Variscan belt, as exemplified by P-T-t-d paths of metabasites in distinct allochthonous units of the Maures massif (SE France). Int J Earth Sci 92:7–26

Bird DK, Cho M, Janik C, Liou JG, Caruso LJ (1988) Compositional order/disorder, and stable isotope characteristics of Al-Fe epidote, state 2–14 drill hole, Salton Sea geothermal system. J Geophys Res 93:13135–13144

Blundy JD, Holland TJB (1990) Calcic amphibole equilibria and a new amphibole-plagioclase geothermometer. Contrib Miner Petrol 104:208–224

Boillot G, Montadert L, Lemoine M, Biju-Duval B (1984) Les marges continentals actuelles et fossils autour de la France. Masson, Paris, 342 pp

Bouillin J, Durand-Delga M, Olivier P (1986) Betic-Rif and Tyrrhenian distinctive features, genesis and development stages. In: Wezel FC (ed) The origin of arcs. Elsevier, Amsterdam, pp 281–304

Bousquet R (2008) Metamorphic heterogeneities within a single HP unit: overprint effect or metamorphic mix? Lithos 103:46–69

Bouybaouène ML (1993) Étude pétrologique des metapelites Sebtides supérieures, Rif Interne, Maroc: Une évolution métamorphique de haute pression. Ph. Thesis. Université Mohammmed V. Rabat, 151 pp

Bouybaouène ML, Goffé B, Michard A (1995) High pressure, low-temperature metamorphism in the Sebtides nappes, northern Rif, Morocco. Geogaceta 17:117–119

Brown EH (1977) The crossite content of Ca-amphiboles as a guide to pressure of metamorphism. J Petrol 18:53–72

Bucher K, Frey M (2002) Petrogenesis of metamorphic rocks. Springer, Berlin, p 341

Carrupt E, Schlup M (1998) Metamorphism and tectonics of the south side of the Val Bognanco (Penninic, Italian). Alps Bul Soc Vaudoise Sci Nat 86:29–59

Chalouan A, Michard A (1990) The Ghomarides nappes, Rif coastal range, Morocco: a variscan chip in the Alpine belt. Tectonics 9:1565–1583

Daczko NR, Caffi P, Halpin JA, Mann P (2009) Exhumation of the Dayman dome metamorphic core complex, eastern Papua New Guinea. J Metam Geol 27:405–422

De Jong K (1991) Tectono-metamorphic studies and radiometric dating in the Betic Cordilleras (SE Spain), with implications for the dynamics of extension and compression in the western Mediterranean area. Tesis Univ, Amsterdam, p 204

De Jong K (1993) The tectono-metamorphic and chronologic development of the Betic Zone (SE Spain) with implications for the geodynamic evolution of the western Mediterranean area. Proc Ned Akad v Wetensch 96:295–333

Desmons J (1989) Different metamorphic evolutions in the Alpine-Apenninic ophiolites (France-Italy-Switzerland-Austria). Chem Geol 77:229–250

Didon J, Durand-Delga M, Kornprobst J (1973) Homologies géologiques entre les deux rives du Détroit de Gibraltar. Bull Soc Géol France 15:77–105

Durand-Delga M (1968) Coup d'oeil sur les unités Malaguides des Cordillères Bétiques (Espagne). C R Acad Sc Paris 266:190–193

Durand-Delga M, Kornprobst J (1963) Esquisse géologique de la région de Ceuta. Bull Soc Géol France 7:1049–1057

Egeler CG (1963) On the tectonics of the eastern Betic Cordilleras (SE Spain). Geol Rundschau 53:260–269

Egeler CG, Simon OJ (1969) Sur la tectonique de la zone Bétique (Cordillères Bétiques Espagne). Ver Kon Ned Akd Wet 25:1–90

Ernst WG, Liu J (1998) Experimental phase-equilibrium study of Al- and Ti-contents of calcic amphibole in MORB-A semiquantitative thermobarometer. Am Miner 83:952–969

Fallot P (1948) Les Cordillères Bétiques. Estudios geol 4:83–172

Fontboté JM, Vera JA (1983) La Cordillera Bética. In: JA Comba (ed) Geología de España. Inst Geol Min España, vol 2, pp 205–343

Frey M, Wieland B (1975) Chloritoid in autochton-parautochton Sedimenten des Aarmassivs. Schweiz Mineral Petrograph Mitt 55:407–418

García-Casco A, Torres-Roldán RL (1996) Disequilibrium induced by fast decompression in St-Bt-Grt-Ky-Sil-And Metapelites from the Betic Belt (Southern Spain). J Petrol 37:1207–1239

García-Dueñas V, Balanyá JC, Martínez Martínez JM (1992) Miocene extensional detachments in the outcropping basement of the northern Alboran basin (Betics) and their implications. Geo Mar Lett 12:88–95

Gerya TV, Perchuk LL, Triboulet C, Audren C, Sez'ko AI (1997) Petrology of the Tumanshet Zonal Metamorphic Complex, Eastern Sayan. Petrology 5(6):503–533

Goffé B, Michard A, García-Dueñas V, González-Lodeiro F, Monié P, Campos J, Galindo-Zaldívar J, Jabaloy A, Martínez-Martínez JM, Simancas F (1989) First evidence of high-pressure, low-temperature metamorphism in the Alpujarride nappes, Betic Cordillera (SE Spain). Eur J Miner 1:139–142

Graham CM, Powell R (1984) A garnet-hornblende geothermometer: calibration, testing, and application to the Pelona Schist, southern California. J Metam Geol 2:13–31

Holland T, Blundy J (1994) Non-ideal interactions in calcic amphiboles and their bearing on amphibole-plagioclase thermometry. Contrib Miner Petrol 116:433–447

Kampschuur W, Rondel HE (1975) The origin of the Betic Orogen Southern Spain. Tectonophysics 27:39–56

Kornprobst J (1974) Contribution à l'étude pétrographique et structurale de la zone interne du Rif (Maroc septentrional). Serv Géol Maroc Mém 25:249

Kornprobst J, Durand-Delga M (1985) Carte géologique du Rif. Sebta. Échelle 1:50000. Feuille NI-30-XIX-4c. Notes Mém Serv Géol Maroc 297

Krenn K, Kaindl R, Hoinkes G (2004) Pumpellyite in metapelites of the Schneeberg Complex (eastern Alps, Austria): a relict of the eo-Alpine prograde P-T path? Eur J Miner 16:661–669

Kretz R (1983) Symbols for rock-forming minerals. Am Miner 68:277–279

Kuhn B, Reuser E, Powell R, Detlef G (2005) Metamorphic evolution of calc-schists in the Central Alps, Switzerland. Schweiz Miner Petrogr Mitt 85:175–190

Laird J, Albee AL (1981) Pressure, temperature, and time indicators in mafic schist: their application to reconstructing the polymetamorphic history of Vermont. Am J Sci 281:127–175

Laird J, Lanphere MA, Albee AL (1984) Distribution of Ordovician and Devonian metamorphism in mafic and pelitic schists from Northern Vermont. Am J Sci 284:376–413

Leake B, Woolley AR, Arps CES, Birch WD, Gilbert MC, Grice JD, Hawthorne FC, Kato FC, Kisch HJ, Krichovichev VG, Linthout K, Laird J, Mandarino JA, Maresch WV, Nickel EH, Rock NMS, Schumacher JC, Smith DC, Stephenson NCN, Ungaretti L, Whittaker EJW, Youzhi G (1997) Nomenclature of amphiboles: report of the subcommittee on amphiboles of the International Mineralogical Association, commission on new minerals and mineral names. Am Miner 82:1019–1037

Mäder UK, Berman RG (1992) Amphibole thermobarometry, a thermodynamic approach. In: Current research, part E. Geological Survey of Canada Paper 92-1E:393–400

Michard A, Goffé B, Bouybaouène ML, Saddiqi O (1997) Late Hercynian-Mesozoic thinning in the Alboran domain: metamorphic data from the northern Rif, Morocco. Terra Nova 9:171–174

Nishimura Y, Coombs D, Landis CA, Itaya T (2000) Continuous metamorphic gradient documented by graphitization and K-Ar age, Southeast Otago, New Zealand. Am Miner 85:1625–1636

Olmo Sanz del A, Pablo Macía de J, Aldaya Valverde F, Campos Fernández J, Chacón Montero J, García Dueñas V, García Rossell L, Sanz de Galdeano C, Orozco Fernández M, Torres Roldán R (1987) Mapa Geológico de España, e:1:50.000, hoja 1064 (Cortes de la Frontera). IGME, 55 pp

Orozco M, Alonso-Chaves FM, Nieto F (1998) Development of large north-facing folds and their relation to crustal extension in the Alborán domain (Alpujarras region, Betic Cordilleras, Spain). Tectonophysics 298:271–295

Platt JP, Vissers RLM (1989) Extensional collapse of thickened continental lithosphere: a working hypothesis for the Alboran Sea and Gibraltar Arc. Geology 17:540–543

Platt J, Soto JI, Comas M (1996) Decompression and high-temperature–low-pressure metamorphism in the exhumed floor of an extensional basin, Alboran Sea, western Mediterranean. Geology 24:447–450

Platt JP, Soto JI, Whitehouse MJ, Hurford AJ, Kelley SP (1998) Thermal evolution, rate of exhumation, and tectonic significance of metamorphic rocks from the floor of the Alboran extensional Basin, Western Mediterranean. Tectonics 17:671–689

Puga E, Díaz De Federico A, Nieto JM (2002a) Tectonostratigraphic subdivision and petrological characterisation of the deepest complexes of the Betic zone: a review. Geodinamica Acta 15:23–43

Puga E, Nieto JM, Díaz De Federico A (2002b) Contrasting P-T paths in eclogites of the Betic Ophiolitic Association, Mulhacén Complex, Southeastern Spain). Can Miner 38:1137–1161

Raase P (1974) Al and Ti contents of hornblende, indicators of pressure and temperature of regional metamorphism. Contrib Miner Petrol 45:231–236

Robinson D, Bevins RE (1999) Patterns of regional low-grade metamorphism in metabasites. In: Frey M, Robinson D (eds) Low-grade metamorphism. Blackwell Science, Oxford, pp 143–168

Robinson P, Spear FS, Schumacher JC, Laird J, Klein C, Evans BW, Doolan BL (1982) Phase relations of metamorphic amphiboles: natural occurrence and theory. Rev Miner 9B:1–227

Ruiz Cruz MD (2010) Zoned Ca-amphibole as new marker of the Alpine metamorphic evolution of phyllites from the Jubrique unit (Alpujárride Complex, Betic Cordillera, Spain). Miner Mag 74:773–796

Ruiz Cruz MD, Rodríguez Jiménez P (2002) Correlation between crystallochemical parameters of phyllosilicates and mineral facies in very low-grade metasediments of the Betic Cordillera (Spain): a synthesis. Clay Miner 37:169–185

Ruiz Cruz MD, Sanz de Galdeano C (2010) Factors controlling the evolution of mineral assemblages and illite crystallinity in Paleozoic to Triassic sequences from the transition between Maláguide and Alpujárride complexes (Betic Cordillera, Spain): the significance of tobelite. Clays Clay Miner 58:558–572

Ruiz Cruz MD, Sanz de Galdeano C, Lázaro C (2005) Metamorphic evolution of Triassic rocks from the transition zone between the Maláguide and Alpujárride complexes (Betic Cordilleras, Spain). Eur J Miner 17:81–91

Ruiz Cruz MD, Franco F, Sanz de Galdeano C, Novak J (2006) Evidence of contrasting low-grade metamorphic conditions from clay mineral assemblages in Triassic Alpujárride-Maláguide transitional units in the Betic Cordilleras, Spain. Clay Miner 41:619–638

Ruiz Cruz MD, Sanz de Galdeano C, Alvarez-Valero A, Rodríguez Ruiz MD, Novak J (2010) Pumpellyite and coexisting minerals in metapelites and veins from the Federico units (Internal Zone of the Rif). Can Miner 48:183–203

Sanz de Galdeano C (1990) Geologic evolution of the Betic Cordilleras in the Western Mediterranean, Miocene to the present. Tectonophysiscs 172:107–119

Sanz de Galdeano C, Andreo B, García-Tortosa FJ, López-Garrido AC (2001) The Triassic palaeogeographic transition between the Alpujárride and Maláguide complexes, Betic-Rif internal zone. Palaeo 167:157–173

Schiffmann P, Day DW (1999) Petrological methods for the study of very low-grade metabasites. In: Frey M, Robinson D (eds) Low-grade metamorphism. Blackwell Science, Oxford, pp 108–142

Schulz B, Triboulet C, Audren C (1995) Microstructures and mineral chemistry in amphibolites from the western Tauern Window (Eastern Alps), and *P-T*-deformation paths of the Alpine greenschists-amphibolite facies metamorphism. Miner Mag 59:641–659

Schulz B, Triboulet C, Audren C, Pfeifer H-R, Gilg A (2001) Two-stage prograde and retrograde Variscan metamorphism of glaucophane-eclogites, blueschists and greenschists from Ile de Groix (Brittany, France). Int J Earth Sci 90:871–889

Schumacher JC (1997) The estimation of the proportions of ferric iron in the electron-microprobe analysis of amphiboles. Can Miner 35:238–246

Schumacher J (2007) Metamorphic amphiboles: composition and coexistence. Rev Miner Geochem 10:359–416

Sharp TG, Buseck PR (1988) Prograde versus retrograde chlorite-amphibole intergrowths in a calc-silicate rock. Am Mineral 73:1292–1301

Simancas JF, Campos J (1993) Compresión NNW–SSE tardi—a postmetamórfica y extensión subordinada en el Complejo Alpujárride (Dominio de Alborán, Orógeno bético). Soc Geol España 6:23–36

Soto JI, Platt JP (1999) Petrological and structural evolution of high-grade metamorphic rocks from the floor of the Alboran Sea basin, Western Mediterranean. J Petrol 40:21–60

Spear FS (1980) NaSi-CaAl exchange equilibrium between plagioclase and amphibole: an empirical model. Contrib Miner Petrol 80:140–146

Theye T, Seidel E, Vidal O (1992) Petrology of carpholite-bearing metapelites and related rocks from the high-pressure metamorphic phyllite-quartzite unit of Crete and Peloponnese (Greece). Eur J Miner 4:487–507

Triboulet C (1992) The (Na-Ca)amphibole-albite-chlorite-epidote-quartz geothermobarometer in the system S-A-F-M-C-N-H_2O. 1. An empirical calibration. J Metam Geol 10:545–556

Tubía JM, Gil Ibarguchi JI (1991) Eclogites of the Ojén nappe: a record of subduction in the Alpujárride complex (Betic Cordilleras, southern Spain). J Geol Soc Lond 148:801–804

Tubía JM, Cuevas J, Navarro-Vilá F, Alvarez F, Aldaya F (1992) Tectonic evolution of the Alpujarride Complex (Betic Cordillera, southern Spain). J Struct Geol 14:193–203

Van Bemmelen MW (1927) Bijdrage tot der geologie der Betische Ketens in der Province de Granada. Ph. D. Thesis, University of Delft

Vidal O, Goffé B, Parra T, Bousquet R (1999) Calibration and testing of an empirical chloritoid-chlorite Mg-Fe thermometer and thermodynamic data for daphnite. J Metam Geol 17:25–39

Vissers RLM, Platt JP, Van der Wal D (1995) Late orogenic extension of the Betic Cordillera and the Alboran Domain: a lithospheric view. Tectonics 14:786–803

Vogl JJ (2003) Thermal-baric structure and P–T history of the brooks range metamorphic core, Alaska. J Metam Geol 21:269–284

Wildi W (1983) La chaîne tello-rifaine (Algérie, Maroc, Tunisie): structure, stratigraphie et évolution du Trias au Miocène. Rev Géol Dyn Geog Phys 24:201–297

Zen E-An (1974) Prehnite- and pumpellyite-bearing mineral assemblages, west side of Appalachian metamorphic belt, Pennsylvania to Newfoundland. J Petrol 15:197–242

Zeck HP, Whitehouse MJ (1999) Hercynian, Pan-African, Proterozoic and Archean ion microprobe zircon ages for a Betic–Rif core complex, Alpine belt, W Mediterranean consequences for its P–T–t path. Contrib Miner Petrol 134:134–149

Zenk M, Schulz B (2004) Zoned Ca-amphiboles and related *P–T* evolution in metabasites from the classical Barrovian metamorphic zones in Scotland. Miner Mag 68:769–786